



**ARTICLE**

# Influence of Recycled Concrete Fine Powder on Durability of Cement Mortar

Yadong Bian<sup>1</sup>, Xuan Qiu<sup>1</sup>, Jihui Zhao<sup>2,\*</sup>, Zhong Li<sup>2</sup> and Jiana Ouyang<sup>2</sup>

<sup>1</sup>School of Architectural and Civil Engineering, Zhongyuan University of Technology, Zhengzhou, 450007, China

<sup>2</sup>School of Civil Engineering, Sun Yat-Sen University & Southern Marine Science and Engineering Guangdong Laboratory (Zhuhai), Zhuhai, 519082, China

\*Corresponding Author: Jihui Zhao. Email: zhaojh28@mail.sysu.edu.cn

Received: 11 February 2023 Accepted: 05 May 2023 Published: 08 November 2023

## ABSTRACT

In this paper, the durability of cement mortar prepared with a recycled-concrete fine powder (RFP) was examined; including the analysis of a variety of aspects, such as the carbonization, sulfate attack and chloride ion erosion resistance. The results indicate that the influence of RFP on these three aspects is different. The carbonization depth after 30 days and the chloride diffusion coefficient of mortar containing 10% RFP decreased by 13.3% and 28.19%. With a further increase in the RFP content, interconnected pores formed between the RFP particles, leading to an acceleration of the penetration rate of CO<sub>2</sub> and Cl<sup>-</sup>. When the RFP content was less than 50%, the corrosion resistance coefficient of the compressive strength of the mortar was 0.84–1.05 after 90 days of sulfate attack. But the expansion and cracking of the mortar was effectively alleviated due to decrease of the gypsum production. Scanning electron microscope (SEM) analysis has confirmed that 10% RFP contributes to the formation of a dense microstructure in the cement mortar.

## KEYWORDS

Recycled concrete fine powder; cement mortar; carbonization; sulfate; chloride ion; durability

## 1 Introduction

At present, with the gradual acceleration of urbanization, the demolition of old buildings has produced lots of construction waste and caused serious environmental pollution problems [1]. The recycling of concrete from construction waste helps to solve the problems associated with the disposal of construction waste and reduces the carbon footprint of the cement concrete industry [2,3]. Large amounts of recycled concrete fine powder (RFP) are produced during the demolition of concrete buildings, and accounts for about 15%–20% of the total waste concrete. The particle size of RFP is small (<0.16 mm), which means that it can be used as a kind of filler in various applications [4–6]. In addition, RFP contains some unreacted cement which has potential reactivity [7,8]. Therefore, RFP could be utilized as a kind of supplementary cementitious material (SCM) to prepare cement-based materials. This is a viable option for the mass utilization of RFP.

Compared to other SCMs, RFP is characterized as cheaper, widely available, and with lower activity. Over the past twenty years, several methods have been used to improve the activity of RFP, including reducing particle size, addition of chemical activator, thermal activation, and mixing with multiple



cementitious materials [9–14]. Alzebaree et al. [15] studied the influence of the fineness of RFP on autoclaved aerated concrete (AAC), and the results showed that finer RFP can effectively enhance the strength of AAC products. In addition, there are also reports in the literature on the influence of RFP on the physical and mechanical properties of recycled cement-based materials [16–18]. According to the research results of Horsakulthai, the compressive strength of self-compacting mortar containing RFP decreases as the percentage of RFP increases and the optimum RFP replacement ratio with a negative effect on the compressive strength is up to 20%. This is consistent with what has been reported elsewhere in the literature [19].

Like mechanical properties, durability is also an important property of cement-based materials and determines the service life of concrete buildings [20,21]. However, there are several problems with the durability of recycled cement-based materials. First, reported studies are relatively scarce as most scholars only focus on a few aspects of durability such that their conclusions are incomplete [22–24]. Second, the research conclusions from different scholars are inconsistent. For these reasons, it is difficult to apply RFP in engineering. In the following paragraph, a brief introduction to the research progress on the durability of recycled cement-based materials is provided.

Khitab et al. [25] investigated the synergistic effect of rubber tires and demolished bricks as a partial replacement for sand and cement in concrete and their results showed that hybrid waste-modified green reactive powder concrete attained good resistance to sodium sulfate attack. Sun et al. [26] used recycled concrete powder (RCP) as a partial replacement of cement in cement mortar at compositions of 0%, 30%, and 50%, respectively, and their test results revealed that RCP content has negative effects and positive effects on the chloride penetration behavior and drying shrinkage respectively. Likes et al. [27] employed the substitution of cement with recycled brick powder (RBP) at 20% in concrete and their results showed that RBP positively impacted on durability, resulting in an increased surface resistivity of 24% over the control. This shows that RBP has the potential for lowering the corrosion rate in reinforced concrete. Sharma et al. [28] used RFP as a partial substitute for fly ash at different replacement levels of 10%, 20%, 30%, 40%, and 50% in fly ash-based geopolymer mortar. Their results showed that the 30% replacement level of RFP in the geopolymer mortar mix showed the maximum decrease in dry shrinkage value. The addition of RFP in the geopolymer mortar mix provided additional N-A-S-H/C-A-S-H gel within the geopolymer matrix which resulted in densifying the microstructure of concrete. Bogas et al. [29] produced concrete with recycled cement (RC) obtained from the thermoactivation of concrete waste (RCCW). Findings from their study indicated that for up to 15% RCCW replacement the concrete durability was not significantly affected. Zhao et al. [30] used recycled brick sand (RBS) as a partial replacement for crushed limestone sand at different levels (0%, 5%, 10%, 25%, and 50%). They reported that due to the higher porosity of the mortar, the RBS can increase the carbonation depth of the mortars and impair the behavior of mortars regarding sulfate attack. However, the apparent chloride diffusion coefficients of mortars made with RBS presented lower values, which means that the mortar made with RBS had better resistance to chloride penetration. Li et al. [31] investigated the properties of RCP and RBP as well as the impact of their incorporation on mortar properties. Their results revealed that the incorporation of high-fineness RBP improved the shrinkage resistance of mortar. The addition of RBP resulted in a refined pore structure by reducing the average pore diameter.

In this paper, carbonization, sulfate erosion, and chloride ion erosion tests on cement mortar containing RFP were carried out to explore the influence of RFP content on the durability of cement mortar. Further, the microstructure of cement mortar containing different RFP contents was evaluated by scanning electron microscopy (SEM) analysis. This work will contribute to the promotion of the application of RFP as a replacement for cement in engineering and increase the added value of RFP.

## 2 Materials and Experimental Methods

### 2.1 Materials and Mortar Specimens

Ordinary Portland cement P.O 42.5 with a specific surface area of  $354 \text{ m}^2/\text{kg}$  was used in this study. The RFP was obtained by crushing, sieving, and grinding the waste concrete from building demolitions. The chemical compositions of the cement and RFP are presented in Table 1, and the particle size distribution of the cement and RFP are shown in Fig. 1. The average particle sizes of the cement and RFP were 22.7 and  $19.3 \mu\text{m}$ , respectively. The X-ray diffraction (XRD) pattern of RFP is shown in Fig. 2. The microstructures of the cement and RFP are shown in Fig. 3. Compared to ordinary silicate cement, the surface of RFP is rough and angular, and the particle size is smaller. RFP contains a large amount of  $\text{SiO}_2$  and some  $\text{CaCO}_3$  with low reactivity. The fine aggregates are standard sand and the mixing water is ordinary tap water.

**Table 1:** Chemical composition of raw materials

	$\text{SiO}_2$	$\text{Al}_2\text{O}_3$	$\text{CaO}$	$\text{Fe}_2\text{O}_3$	$\text{MgO}$	$\text{Na}_2\text{O}$	$\text{SO}_3$
Cement	20.6	5.1	63.3	3.4	2.0	0.6	2.06
RFP	60.3	10.4	17.4	3	3.4	2.1	0.7

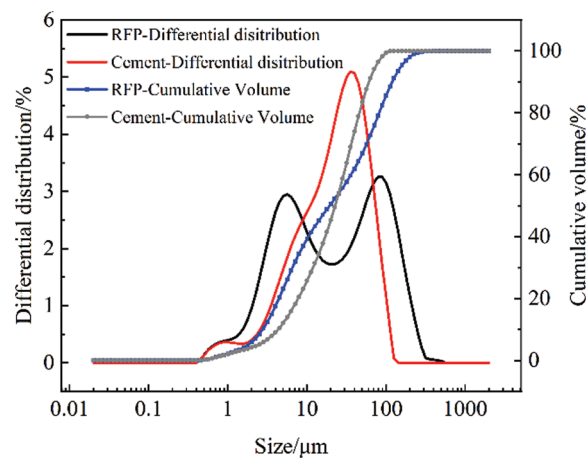


**Figure 1:** Particle size distribution of RFP and cement

Four RFP contents for the cement mortar were considered, and the detailed mix proportions are presented in Table 2. The process of preparation of the mortar is as follows. Firstly, water and cement were poured into the mixing pot, and the mixture was stirred at low speed for 1 min; then sand was added into mixture. Finally, the mixture was stirred at high speed for 90 s. The fresh mortar was poured into a mold and vibrated to form. After 24 h, the samples were demolded. All concrete specimens were cured for 28 days in a standard environment at a temperature of  $20^\circ\text{C}$  and relative humidity of 95%.

### 2.2 Experimental Methods

#### 2.2.1 Compressive and Flexural Strength Tests

The compressive and flexural strength tests on the recycled mortar were carried out according to a standard method, GB/T 17671–1999 (Method of testing cements-Determination of strength). The test

block used for flexural strength was a cube test block of  $40\text{ mm} \times 40\text{ mm} \times 160\text{ mm}$  size, and the compressive strength was carried after fracture resulting from the flexural test.

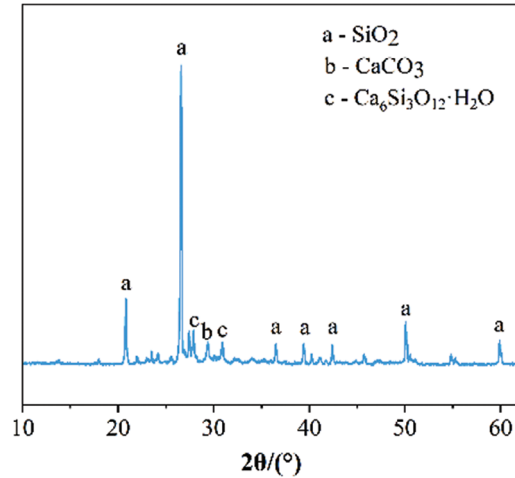


**Figure 2:** XRD pattern of RFP

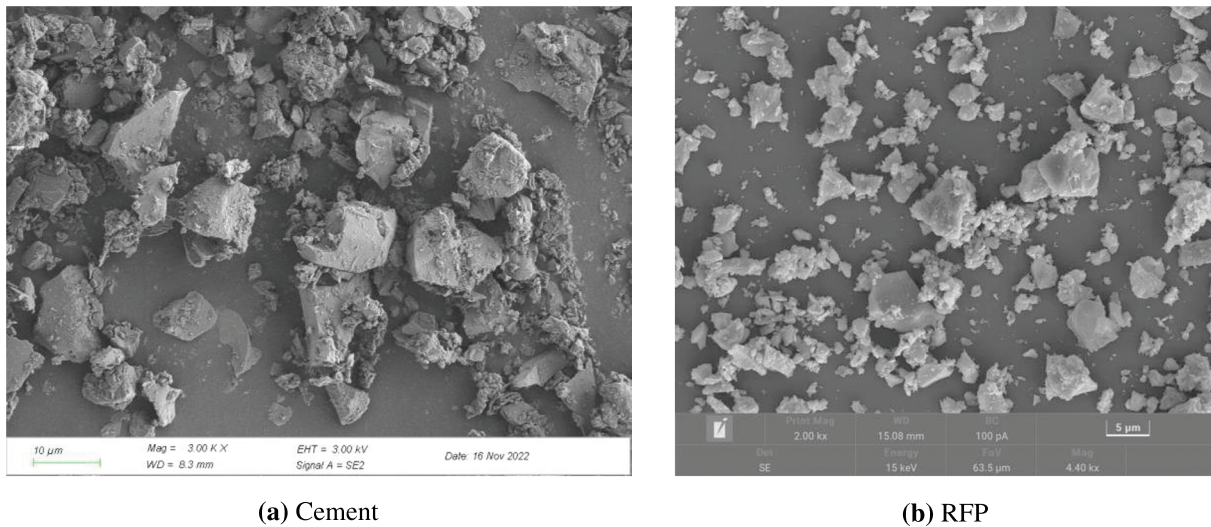


**Figure 3:** Micro-morphology of cement and RFP

### 2.2.2 Carbonation Test

The specimens were cured for 28 days and then carbonated in a carbonation chamber at a temperature of  $20^\circ\text{C} \pm 2^\circ\text{C}$ , a relative humidity of  $70\% \pm 5\%$  and a  $\text{CO}_2$  concentration of  $20\% \pm 3\%$ . The carbonation ages were 15, 30, and 45 days, respectively. At the corresponding carbonation age, phenolphthalein indicator was sprayed on the section of the test block and the area on the section that did not turn red was measured with vernier calipers and averaged over eight points to calculate the depth of carbonation.

### 2.2.3 Chloride Ion Erosion Test

The chloride ion rapid electromigration method and the electric flux method were used for the tests, respectively. The rapid electromigration of chloride ions was determined using the RCM-NTB chloride

ion diffusion coefficient tester and the electric flux method was carried out using the NEL-PEU concrete electric flux tester with a determination time of 6 h.

**Table 2:** Mix proportions of mortar samples

Specimen	RFP content (%)	RFP content (g)	Cement (g)	Sand (g)	Water (g)
RFP0	0	0	450	1350	225
RFP10	10	45	405	1350	225
RFP30	30	135	315	1350	225
RFP50	50	225	225	1350	225

#### 2.2.4 Sulphate Attack Test

According to the GB/T 50082-2009 “Standard for long-term performance and durability test methods for ordinary concrete”, a 5% sodium sulphate solution was used to soak the sample specimens cured for 28 days for 30, 60, and 90 days. The sulphate attack resistance of the recycled mortar was evaluated by the corrosion resistance coefficient of compressive strength, the corrosion resistance coefficient of flexural strength, and mass change rate of the specimens at different soaking ages. The corrosion resistance coefficient of compressive strength and the corrosion resistance coefficient of flexural strength were calculated according to Eqs. (1) and (2), respectively:

$$R_c = \frac{f_{cn}}{f_{c28}} \quad (1)$$

$$R_f = \frac{f_{fn}}{f_{f28}} \quad (2)$$

where  $R_c$  is the corrosion resistance coefficient of compressive strength;  $f_{cn}$  is the compressive strength of the specimen at each erosion age;  $f_{c28}$  is the compressive strength of the specimen at 28 days of curing;  $R_f$  is the corrosion resistance coefficient of flexural strength;  $f_{fn}$  is the flexural strength of the specimen at each erosion age;  $f_{f28}$  is the flexural strength of the specimen at 28 days of curing.

The rate of mass change of specimen was calculated according to Eq. (3):

$$W_t = \frac{G_1 - G_0}{G_0} \times 100\% \quad (3)$$

where  $W_t$  is the rate of mass change of specimen;  $G_0$  is the mass of specimen before erosion;  $G_1$  is the mass of specimen after erosion.

#### 2.2.5 Microstructure Analysis

A thin slice sample was taken from the broken test block after the compressive strength test was finished. The sample was placed in a centrifuge tube and an appropriate amount of absolute ethyl alcohol was poured into the tube to terminate the sample's hydration; this process lasted for 12 h. Then the sample was dried in a drying oven for 12 h. The surface of the dried sample was sprayed with gold and the microscopic morphology was observed by SEM. The scanning electron microscope used is the Zeiss Sigma 300, set to the secondary electron mode.

### 3 Results and Discussion

#### 3.1 The Strength Activity Index of RFP

The strength activity index of the RFP and the compressive strength of the recycled mortar are shown in Figs. 4 and 5, respectively. The activity index of the RFP and compressive strength of the recycled mortar significantly decreased with increasing RFP content. The compressive strength of mortar was reduced by 0.91%, 24.15%, and 53.3%, respectively when RFP content was 10%, 30%, and 50%. This indicates that when the RFP content is less than 10%, the compressive strength of recycled mortar is not noticeably affected by RFP. The filling effect and low reactivity has a positive and a negative effect on the compressive strength of mortar, respectively. When RFP content is less than 10%, the two effects cancel each other out; when RFP content is more than 30%, the generation of hydration products is greatly reduced, which means that the positive effect is much lower than negative effect, thus leading to the compressive strength being significantly decreased.

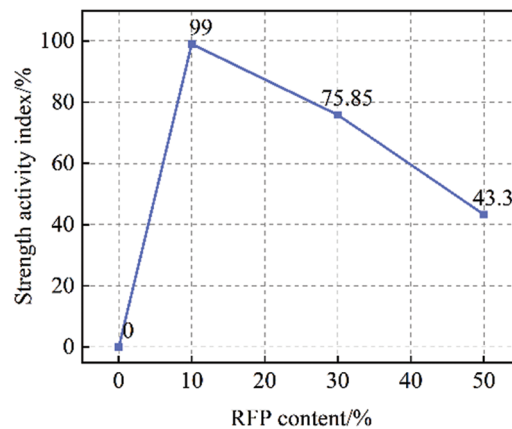


**Figure 4:** Strength activity index of RFP

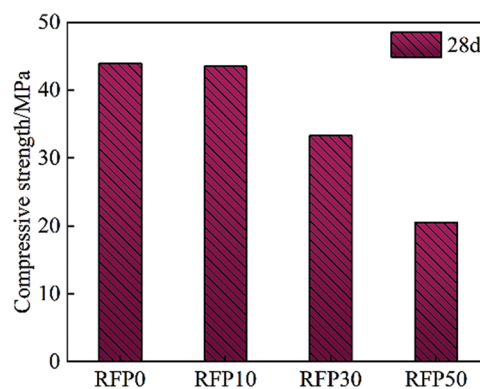


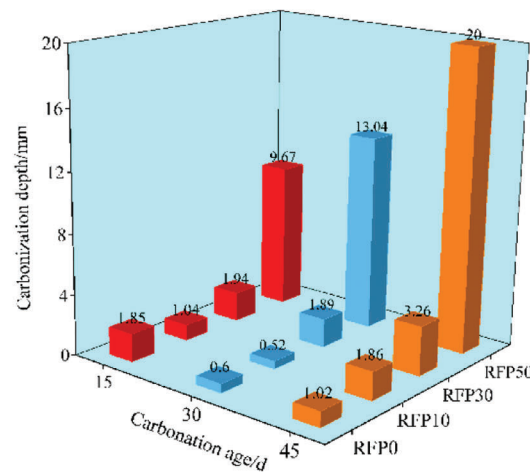
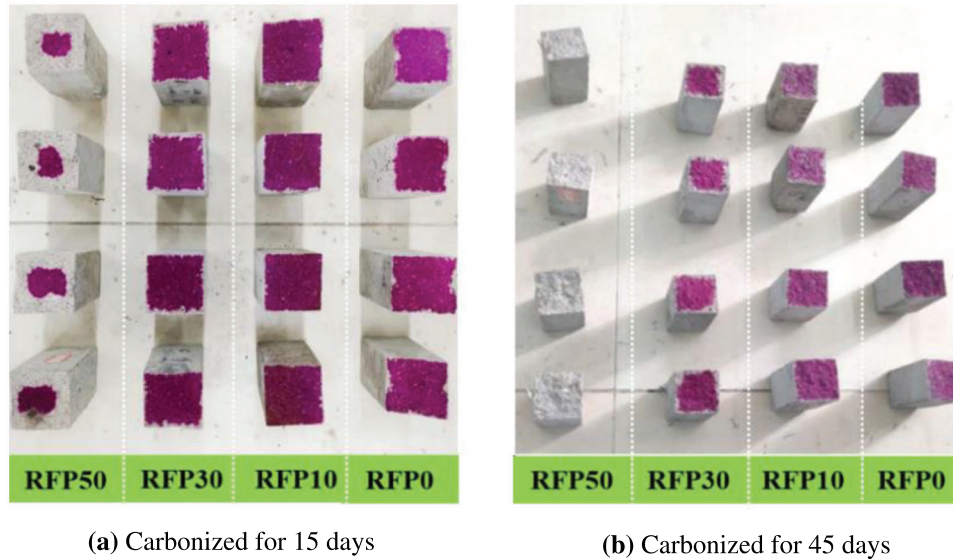
**Figure 5:** Compressive strength of recycled mortar

#### 3.2 Carbonization Resistance of Recycled Mortar

Fig. 6 shows the carbonation depth of the recycled mortar at different carbonation ages. A 10% RFP content reduces the carbonation depth of mortar at an early carbonation age. Compared to RFP0, the carbonation depth of RFP10 decreased by 43.8% and 13.33% at 15 and 30 days, respectively (see



Fig. 6c). At 45 days of carbonation, the carbonation depth of the recycled mortar increased with the RFP content, and the RFP50 has been completely carbonized. This indicates that RFP can improve the carbonization resistance of mortar in the early stage of carbonization. However, RFP has a negative effect on the carbonization resistance of mortar in the late stage of carbonization.



(c) Carbonization depth

**Figure 6:** The carbonization depth of recycled mortar at different carbonation ages

The main reason for the increasing carbonation depth of recycled mortar is that  $\text{CO}_2$  reacts with  $\text{Ca}(\text{OH})_2$  (CH) and C-S-H gel. Three reactions occur simultaneously in the process of carbonization of recycled mortar. The first is the carbonization of hydration products. The second is the hydration reaction of unreacted cement particles. And the last is the pozzolanic reaction of RFP. In the early stage of carbonization, only a part of the hydration products produced are carbonized. As the carbonization process continues, the hydration products increase and the generated hydration products are gradually carbonized. When a certain age is reached, the potential activity of RFP comes into play, and a part of the CH generated by cement hydration will be used for the pozzolanic reaction, such that the component will be reduced (possibly by carbonization). Appropriate amounts of RFP can fill the voids within the mortar

to stop  $\text{CO}_2$  from permeating. When the RFP content is further increased, the hydration products are reduced, and the compactness of the matrix is decreased. Meanwhile, connected pores are formed between the accumulated RFP particles due to their being loose, thus enhancing diffusion of  $\text{CO}_2$ . Therefore, the carbonization resistance of recycled mortar is greatly reduced.

Fig. 7 shows the compressive strength and flexural strength of recycled mortar at different carbonization ages. The strength of recycled mortar gradually increased with carbonation age. After 45 days of carbonization, the compressive strength of RFP0, RFP10, RFP30, and RFP50 increased by 17.8%, 15.4%, 36.3%, and 50.2%, respectively, and the flexural strength increased by 31.4%, 44.6%, 32.8%, and 46.3%, respectively. The strength of recycled mortar gradually decreased with the increase of RFP. After 45 days of carbonization, the compressive strength of RFP10, RFP30, and RFP50 was reduced by 2.9%, 12.2%, and 40.4%, while the flexural strength was reduced by 5.3%, 21.2%, and 30.1% compared with RFP0.

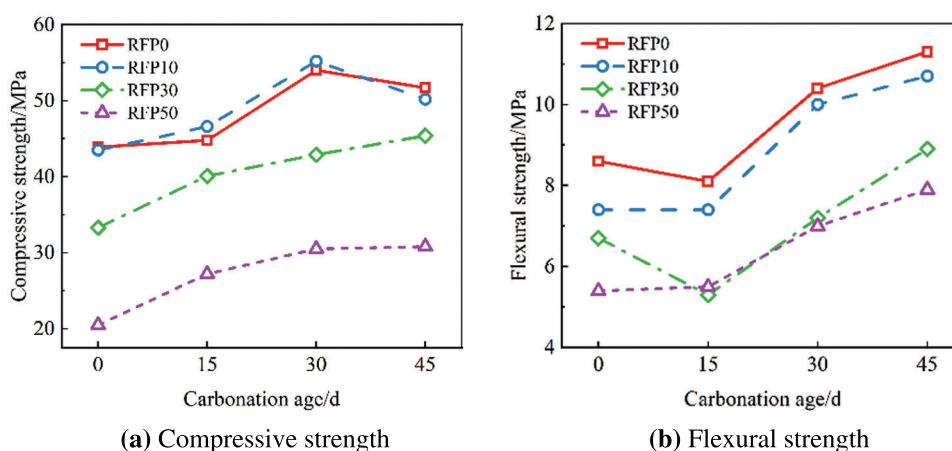


**Figure 7:** Mechanical properties of recycled mortar at different carbonization ages

There are two reasons for the improvement in strength of recycled mortar after carbonization. On the one hand, the hydration reaction of cement continues in the carbonization process and hydration products are increasing; on the other hand, the carbonization product  $\text{CaCO}_3$  improves the internal compactness of recycled mortar. The change rule of compressive strength of RFP0 and RFP10 is similar, which is related to the similar cement hydration product  $\text{Ca}(\text{OH})_2$  content of these two groups. For RFP30 and RFP50, the amount of cement was greatly reduced so the hydration products decreased. As a result, the compactness of the matrix decreased. With the development of carbonation age,  $\text{CaCO}_3$  gradually filled the pores and contributed to strength and hardness for the matrix. Therefore, the compressive strength of RFP30 and RFP50 increased steadily.

### 3.3 Sulfate Attack Resistance of Recycled Mortar

The mechanical properties of the recycled mortar at different ages of sulfate attack are shown in Fig. 8. As shown in Figs. 8a and 8c, both the compressive and flexural strengths of the recycled mortar first increased and then decreased with age. The compressive strength of the recycled mortar reached a maximum at 60 days, with RFP0, RFP30, and RFP50 increasing by 24.6%, 38%, and 33.6%, respectively. The flexural strength of the recycled mortar reached a maximum at 30 days, with RFP0, RFP10, RFP30, and RFP50 increasing by 12.8%, 32.4%, 29.9%, and 35.2%, respectively. Compared with the unaged sample (0 day), the compressive strength of RFP10 increased by 6.89% at 30 days of erosion, and decreased by 11.5% and 15.6% at 60 and 90 days of erosion, respectively. According to the rule of compressive strength of the other three groups, it can be deduced that the compressive strength will decrease after 90 days. Similar conclusions were made in the study by Cheng et al. [32]. The decline of compressive strength in



RFP10 happened earlier compared with the other groups. As shown in Figs. 8b and 8d, the  $R_c$  and  $R_f$  of the recycled mortar showed little change compared with RFP0 at 90 days, for which the  $R_c$  and  $R_f$  ranged from 0.84 to 1.05 and 0.78 to 1.35. This indicates that RFP has little effect on the sulfate attack resistance of cement mortar.

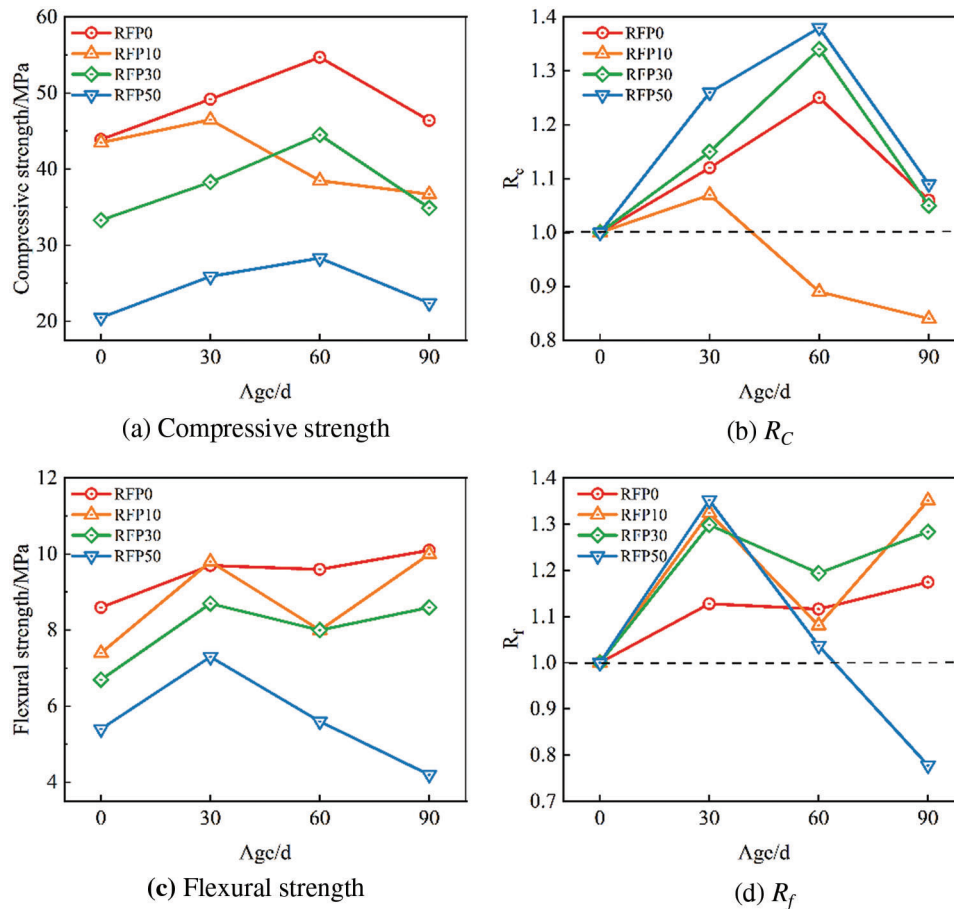


**Figure 8:** The mechanical properties of recycled mortar at different corrosion ages

Fig. 9 shows the rate of mass change of the recycled mortar at different sulfate attack ages. The mass of specimen first increased and then decreased with the erosion age. The mass of RFP0, RFP10, RFP30, and RFP50 increased by 0.33%, 0.35%, 0.19%, and 0.13%, respectively. The mass of RFP30 and RFP50 decreased by 0.04% at 30 days. In addition, at different sulfate attack ages, the influence rule of RFP on the mass of the recycled mortar was significantly different. At 60 days of age, the rate of mass change of the recycled mortar decreased with the increase of RFP content. At 90 days of age, the rate of mass change of the recycled mortar gradually increased with RFP content.

In the sulfate immersion environment, the change of strength and mass of recycled mortar is mainly related to the transformation of AFt, the formation of gypsum, and the expansion and cracking of the matrix. In the early age of sulfate immersion, the mass and strength of specimen is improved due to the void of matrix possibly being filled by AFt and gypsum. With increasing erosion age, the cement hydration reaction continued, the amount of  $\text{Ca}^{2+}$ , AFt, and gypsum gradually increased, and the strength and rate of mass change increased accordingly. In the late age of sulfate immersion, the cement matrix

expands and cracks due to excessive Aft and gypsum formation. Therefore, the strength and mass of specimen began to decrease. In this process, RFP delayed the cement hydration process and reduced the gypsum content. Moreover, with increasing RFP content, there is an obvious trend of decreasing strength and mass.

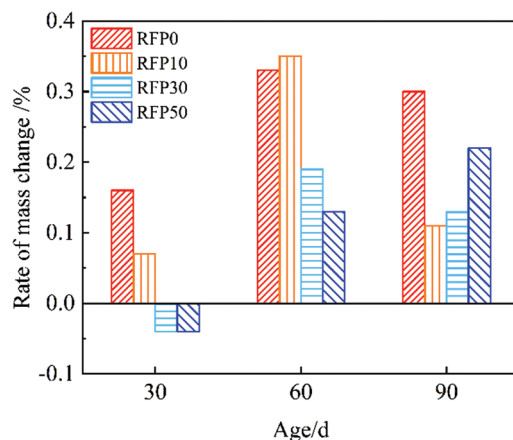


**Figure 9:** Rate of mass change of recycled mortar at different corrosion ages

### 3.4 Chloride Ion Erosion Resistance of Recycled Mortar

Fig. 10 shows the electric flux and chloride diffusion coefficient of recycled mortar. Both the electric flux and chloride diffusion coefficient of RFP10 were lower than RFP0, which indicates that 10% RFP can improve the chloride ion erosion resistance of recycled mortar. However, when the RFP content exceeds 10%, RFP has a negative effect on the chloride ion resistance of recycled mortar. Appropriate amounts of RFP can enhance its filling effect and pozzolanic effect to improve the pore structure of recycled mortar. In addition, due to RFP having much amorphous  $\text{Al}_2\text{O}_3$ ,  $\text{Si}^{2+}$  is replaced by  $\text{Al}^{3+}$  in the C-S-H gel and makes the silico-oxygen tetrahedron charge unbalanced and negatively charged. Cations form an adsorption layer on the surface of the silico-oxygen tetrahedron, and a diffusion layer formed by anions such as  $\text{Cl}^-$  and  $\text{OH}^-$  is formed outside the adsorption layer, which together constitute a double electric layer. Thus, the curing ability of mortar for  $\text{Cl}^-$  is improved [14]. Therefore, the chloride ion erosion resistance of recycled mortar has been improved due to these three aspects. When the RFP content is excessive, hydration products are significantly reduced, while the connected pores which are formed among the RFP particles will accelerate the diffusion of chloride ions.

### 3.5 SEM Analysis

Fig. 11 shows the influence of RFP on the microstructure of cement mortar. There were more fibrous C-S-H gel and an appropriate amount of flake CH in the mortar without RFP (see Fig. 11a). When 10% RFP was added, the C-S-H gel further increased and CH significantly decreased, which indicates that the RFP consumed a part of CH and generated C-S-H gel, with the microstructure becoming denser at the same time (see Fig. 11b). As the RFP content gradually increased, C-S-H gel was difficult to increase and there remained a small amount of unreacted RFP particles on the surfaces of the hydration products. This indicates that a large amount of CH generated by cement hydration has been consumed, and the remaining RFP particles were not involved in secondary hydration but only acted as inert fillers (see Fig. 11c). When the RFP content was 50%, the CH production decreased significantly and was completely consumed by RFP. A large number of unreacted RFP particles were distributed around the

hydration products, meanwhile, the microstructure was loose and porous and the degree of compactness was decreased (see Fig. 11d).

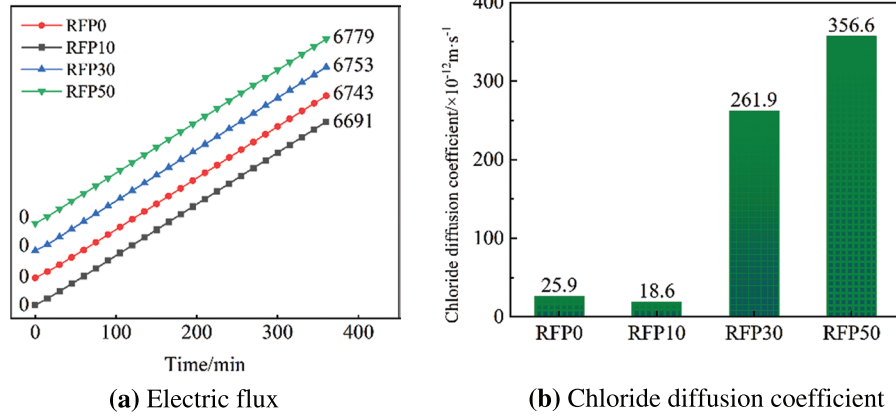


Figure 10: Electric flux and chloride diffusion coefficient of recycled mortar

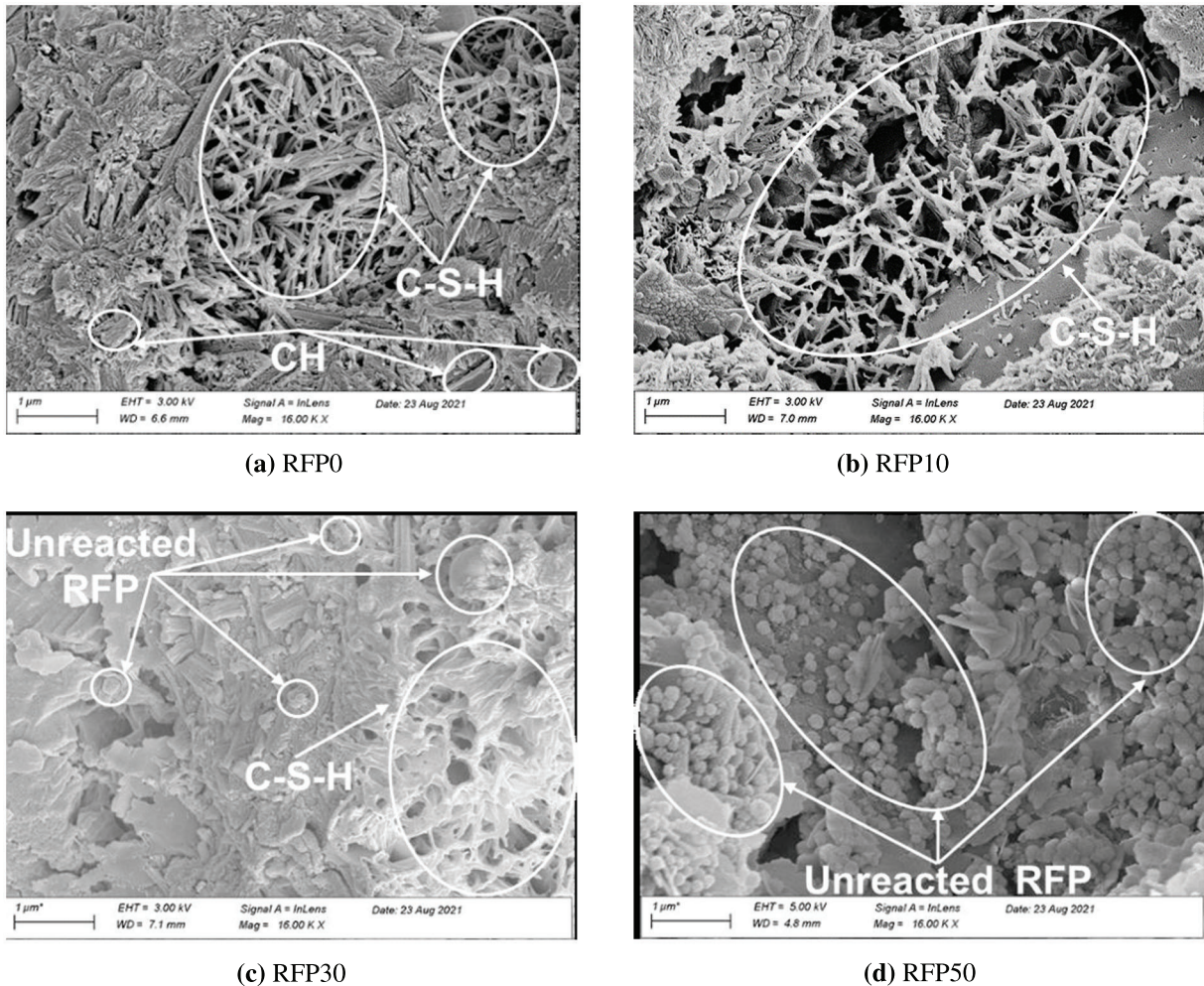


Figure 11: SEM images of recycled mortar

## 4 Conclusions

Based on the findings of the study, the following conclusions are drawn:

(1) At 45 days of carbonization, the carbonization resistance of cement mortar decreases with the increase of RFP. Compared with RFP0, the carbonization depth of RFP10 and RFP30 is increased by 0.8 and 2.2 times, respectively and RFP50 is fully carbonized. Due to the characteristics of the porous surface of RFP particles, more interconnected pores will be formed when a large amount of RFP particles are accumulated. Furthermore, the number of interconnected pores increase with the RFP content, thus the rate of penetration of CO<sub>2</sub> is accelerated.

(2) After 90 days of sulfate attack, the  $R_c$  and  $R_f$  of mortar are 0.84–1.05 and 0.78–1.35, respectively. Essentially, RFP content less than 50% has little effect on the sulfate attack resistance of cement mortar. The deterioration of mortar performance is caused by the increase of gypsum in the sulfate environment. Although the microstructure of mortar become loose when a large amount of RFP is added, the CH production decreases and part of the CH is consumed by RFP, which leads to a decrease in gypsum production. As a result, the expansion and cracking of mortar is effectively alleviated.

(3) The chloride ion erosion resistance of cement mortar is improved by 10% RFP and the electric flux and chloride diffusion coefficient reduced by 0.77% and 28.19% respectively. A 10% RFP content can contribute to forming a dense microstructure in cement mortar and reducing the penetration of chloride ion.

**Acknowledgement:** This study would not have materialized but for the numerous support and encouragement we have received from many parties. The authors would like to take this opportunity to express our heartfelt gratitude to all who have assisted us.

**Funding Statement:** This work is supported by the Zhuhai Science and Technology Project (ZH22036203200015PWC) and the Open Foundation of State Key Laboratory of Subtropical Building Science (2022ZB20).

**Author Contributions:** Yadong Bian: Conceptualization, methodology. Xuan Qiu: Writing, formal analysis. Jihui Zhao: Review & editing. Zhong Li: Writing original draft. Jiana Ouyang: Investigation, preparation.

**Availability of Data and Materials:** All data is presented in this research.

**Conflicts of Interest:** The authors declare that they have no conflicts of interest to report regarding the present study.

## References

1. Zhang, A., Lu, M. (2022). Analysis of highway asphalt modified with recycled rubber and waste plastics. *Fluid Dynamics & Materials Processing*, 18, 907–918. <https://doi.org/10.32604/fdmp.2022.018995>
2. Long, Y., Wang, J. (2021). A study on the strength surplus coefficient of cement. *Fluid Dynamics & Materials Processing*, 17, 181–187. <https://doi.org/10.32604/fdmp.2021.011185>
3. Wu, Z., Wu, Y., Xie, R., Yang, J., Liu, S. et al. (2023). Analysis of the microstructure of a failed cement sheath subjected to complex temperature and pressure conditions. *Fluid Dynamics & Materials Processing*, 19, 399–406. <https://doi.org/10.32604/fdmp.2022.020402>
4. Li, Z., Bian, Y., Zhao, J., Wang, Y., Yuan, Z. (2022). Recycled concrete fine powder (RFP) as cement partial replacement: Influences on the physical properties, hydration characteristics, and microstructure of blended cement. *Journal of Building Engineering*, 62, 105326. <https://doi.org/10.1016/j.job.2022.105326>
5. Bian, Y., Li, Z., Zhao, J., Wang, Y. (2022). Synergistic enhancement effect of recycled fine powder (RFP) cement paste and carbonation on recycled aggregates performances and its mechanism. *Journal of Cleaner Production*, 344, 130848. <https://doi.org/10.1016/j.jclepro.2022.130848>



6. Moon, D. J., Kim, Y. B., Ryou, J. S. (2008). An approach for the recycling of waste concrete powder as cementitious materials. *Journal of Ceramic Processing Research*, 9, 278–281.
7. Li, S., Gao, J., Li, Q., Zhao, X. (2021). Investigation of using recycled powder from the preparation of recycled aggregate as a supplementary cementitious material. *Construction and Building Materials*, 267, 120976. <https://doi.org/10.1016/j.conbuildmat.2020.120976>
8. Liu, M., Wang, C., Wu, H., Yang, D., Ma, Z. (2022). Reusing recycled powder as eco-friendly binder for sustainable GGBS-based geopolymer considering the effects of recycled powder type and replacement rate. *Journal of Cleaner Production*, 364, 132656. <https://doi.org/10.1016/j.jclepro.2022.132656>
9. Kim, J., Jang, H. (2022). Closed-loop recycling of C&D waste: Mechanical properties of concrete with the repeatedly recycled C&D powder as partial cement replacement. *Journal of Cleaner Production*, 343, 130977. <https://doi.org/10.1016/j.jclepro.2022.130977>
10. Mukai, K., Pereslavtsev, P., Fischer, U., Knitter, P. (2015). Activation calculations for multiple recycling of breeder ceramics by melt processing. *Fusion Engineering and Design*, 100, 565–570. <https://doi.org/10.1016/j.fusengdes.2015.08.007>
11. Ren, P., Li, B., Yu, J., Ling, T. (2022). Utilization of recycled concrete fines and powders to produce alkali activated slag concrete blocks. *Journal of Cleaner Production*, 267, 122115. <https://doi.org/10.1016/j.jclepro.2020.122115>
12. Sasui, S., Kim, G., Nam, J., Alam, S. F., Eu, H. et al. (2023). Alkali activation of waste concrete powder: Effects of alkali type and concentration. *Ceramics International*, 49, 16260–16271. <https://doi.org/10.1016/j.ceramint.2023.01.224>
13. Topic, J., Fladr, J., Prosek, Z. (2017). Flexural and compressive strength of the cement paste with recycled concrete powder. *Advanced Materials Research*, 1144, 65–69. [www.scientific.net/AMR.1144.65](http://www.scientific.net/AMR.1144.65)
14. Abed, M., Names, R. (2019). Long-term durability of self-compacting high-performance concrete produced with waste materials. *Construction and Building Materials*, 212, 350–361. <https://doi.org/10.1016/j.conbuildmat.2019.04.004>
15. Alzebaree, R., Mawlod, A. O., Mohammedameen, A., Nis, A. (2021). Using of recycled clay brick/fine soil to produce sodium hydroxide alkali activated mortars. *Advances in Structural Engineering*, 24, 2996–3009. <https://doi.org/10.1177/13694332211015742>
16. Pavlu, T., Sefflova, M. (2016). The development of the fine-aggregate concrete strength with recycled cement powder. *Applied Mechanicals and Materials*, 827, 255–258. <https://doi.org/10.4028/www.scientific.net/AMM.827.255>
17. Kim, H. S., Lee, S. H., Kim, B. (2017). Properties of extrusion concrete panel using waste concrete powder. *Applied Sciences*, 7, 910. <https://doi.org/10.3390/app7090910>
18. Larsen, Q., Samchenko, S., Naruts, V. (2022). Blended binder based on Portland cement and recycled concrete powder. *Magazine of Civil Engineering*. <https://doi.org/10.34910/MCE.113.6>
19. Horsakulthai, V. (2021). Effect of recycled concrete powder on strength, electrical resistivity, and water absorption of self-compacting mortars. *Case Studies in Construction Materials*, 15, e00725. <https://doi.org/10.1016/j.cscm.2021.e00725>
20. Taherkhani, H., Bayat, R. (2020). Investigating the properties of asphalt concrete containing recycled brick powder as filler. *European Journal of Environmental and Civil Engineering*, 26, 3583–3593. <https://doi.org/10.1080/19648189.2020.1806932>
21. Baldovino, J., Lzzo, R., Rose, J., Domingos, M. (2021). Strength, durability, and microstructure of geopolymers based on recycled-glass powder waste and dolomitic lime for soil stabilization. *Construction and Building Materials*, 271, 121874. <https://doi.org/10.1016/j.conbuildmat.2020.121874>
22. Liu, X., Liu, R., Xie, X., Zuo, J., Lyu, K. et al. (2023). Chloride corrosion resistance of cement mortar with recycled concrete powder modified by nano-silica. *Construction and Building Materials*, 364, 129907. <https://doi.org/10.1016/j.conbuildmat.2022.129907>
23. Gao, Y., Cui, X., Lu, N., Hou, S., He, Z. et al. (2022). Effect of recycled powders on the mechanical properties and durability of fully recycled fiber-reinforced mortar. *Journal of Building Engineering*, 45, 103574. <https://doi.org/10.1016/j.jobbe.2021.103574>



24. Bai, H., Li, Y., Dai, D. (2022). Study on the durability of recycled powder concrete against sulfate attack under partial immersion condition. *Journal of Renewable Materials*, 10, 3059–3078. <https://doi.org/10.32604/jrm.2022.020148>
25. Khitab, A., Kirgiz, M. S., Nehdi, M. L., Mirza, J., Galdino, A. G. D. et al. (2022). Mechanical, thermal, durability and microstructure behavior of hybrid waste-modified green reactive powder concrete. *Construction and Building Materials*, 344, 128184. <https://doi.org/10.1016/j.conbuildmat.2022.128184>
26. Sun, C., Chen, L., Xiao, J., Singh, A., Zeng, J. (2021). Compound utilization of construction and industrial waste as cementitious recycled powder in mortar. *Resources, Conservation & Recycling*, 170, 105561. <https://doi.org/10.1016/j.resconrec.2021.105561>
27. Likes, L., Markandeya, A., Haider, M. M., Bollinger, D., McCloy, J. S. et al. (2022). Recycled concrete and brick powders as supplements to Portland cement for more sustainable concrete. *Journal of Cleaner Production*, 364, 132651. <https://doi.org/10.1016/j.jclepro.2022.132651>
28. Sharma, A., Singh, P., Kapoor, K. (2022). Utilization of recycled fine powder as an activator in fly ash based geopolymer mortar. *Construction and Building Materials*, 323, 126581. <https://doi.org/10.1016/j.conbuildmat.2022.126581>
29. Bogas, J. A., Carrica, A., Real, S. (2022). Durability of concrete produced with recycled cement from waste concrete. *Materials Today: Proceedings*, 58, 1149–1154. <https://doi.org/10.1016/j.matpr.2022.01.280>
30. Zhao, Z., Xiao, J., Duan, Z., Hubert, J., Grigoletto, S. et al. (2020). Performance and durability of self-compacting mortar with recycled sand from crushed brick. *Journal of Building Engineering*, 57, 104867. <https://doi.org/10.1016/j.jobbe.2022.104867>
31. Li, S., Gao, J., Li, Q., Zhao, X. (2021). Investigation of using recycled powder from the preparation of recycled aggregate as a supplementary cementitious material. *Construction and Building Materials*, 267, 120976. <https://doi.org/10.1016/j.conbuildmat.2020.120976>
32. Cheng, H., Liu, T., Zou, D., Zhou, A. (2021). Compressive strength assessment of sulfate-attacked concrete by using sulfate ions distributions. *Construction and Building Materials*, 293, 123550, <https://doi.org/10.1016/j.conbuildmat.2021.123550>